

# The nonlinear elasticity of an $\alpha$ -helical polypeptide: Monte Carlo studies

Buddhapriya Chakrabarti\* and Alex J. Levine<sup>†</sup>  
*Department of Physics, University of Massachusetts,  
Amherst, MA 01003*

(Dated: November 2, 2018)

We perform Monte Carlo simulations to study the elastic properties of the helix-coil worm-like chain model of alpha-helical polypeptides. In this model the secondary structure enters as a scalar (Ising like) variable that controls the local chain bending modulus. We compute numerically the bending and stretching compliances of this molecule as well as the nonlinear interaction between stretching and torque over a wide range of model parameters. The numerical results agree well with previous mean-field and perturbative calculations where they are expected to do so. The Monte Carlo simulations allow us to examine the response of the chain to large forces and torques where the perturbative approaches fail. In addition we extend our mean-field analysis by studying the fluctuation dominated regime at the force-induced denaturation transition.

PACS numbers: 87.10.+e,87.14.Ee,82.35.Lr

## I. INTRODUCTION

The mechanical properties of semiflexible biopolymers such as F-actin are well described by the worm-like chain Hamiltonian[1, 2], which treats the filament as a one dimensional elastic continuum without internal structure. Experiments based on single molecule manipulations[3, 4, 5, 6, 7, 8, 9, 10] have demonstrated the essential validity of this coarse-grained approach to the investigation of biopolymer statistics and mechanical properties. Understanding both scattering function of such semiflexible polymers in dilute solution[11] and the force extension relations[12] of single semiflexible polymers are among the principal successes of this coarse-grained description of these polymers. A simplification of this nature, although valid in numerous contexts, must breakdown under forces that are large enough to modify the local structure of the polymer. For example the worm-like chain Hamiltonian ignores the double helical structure of DNA and the local secondary structure of polypeptides. This local molecular structure controls the bending modulus of the polymer and can be disrupted under applied stress. This limitation of the worm-like chain (WLC) model is becoming increasingly apparent as researchers probe the mechanical properties of biopolymers under larger applied forces where such a coupling between local molecular structure and chain elasticity plays an important role [13]. Such large forces are not only experimentally accessible but are also biologically relevant in such processes as those associated with DNA looping[14, 15] and in protein conformational change. An example of the latter process can be found in the conformational change of the protein Calmodulin that involves the buckling of a single, solvent-exposed alpha-helical domain upon the binding of  $\text{Ca}^{2+}$  ions[16, 17]. A polymer

model of the alpha-helical domain that incorporates this nonlinear elastic response of the chain is therefore required to explore conformation change. We expect that such a model (as presented here) will be broadly applicable to the investigation of protein allostery.

Recently we[18, 19] and others[15, 20] proposed a minimal extension of worm-like chain called the helix/coil worm-like chain (HCWLC) to describe biopolymers with internal structure. This model couples the conformational degrees of freedom of the polymer backbone to localized structural transitions of the constituent monomers by postulating that the local bending modulus of the worm-like chain depends on the local degree of internal structure (the helix/coil variable). For example, the bending modulus of an alpha-helical polypeptide depends on the local presence of secondary structure and the consequent hydrogen bonding that effectively stiffens the chain. The fundamental result of this coupling is to make both the torque and force response of the polymer highly nonlinear due to localized denaturation events (loss of local secondary structure) under mechanical stress. These denatured regions introduce more compliant elements into the chain leading to abrupt changes in the effective moduli of the polymer at a critical applied stress.

It is important to note that the secondary structure variables are locally coupled along the chain since the alpha-helical structure is stabilized by hydrogen bonding between adjacent turns of the helix. These nearest neighbor interactions between the secondary structure variables make the denaturation transition cooperative. We will parameterize this cooperativity by an energy scale in what follows referring to it as the chain cooperativity parameter. The worm-like chain Hamiltonian and our extension of it, the HCWLC are discussed in more detail in section II.

The numerical work reported here complements our previous analytic calculations of the extension and bending compliances of alpha-helical polypeptides as modelled within the framework of the HCWLC. For the case of ex-

---

\*Electronic address: buddho@physics.umass.edu

<sup>†</sup>Electronic address: levine@physics.umass.edu

ternally applied torques with no externally applied tensile stress, these analytic calculations have been carried out exactly. Both the force extension relations of the molecule and the nonlinear coupling of the extensional compliance to the state of torque, however, cannot be solved in closed form. A similar issue arises in the study of the extensional compliance of the worm-like chain[12]. Previously we examined the response of the molecule to tensile stress as well as to a combination of torque and tensile stress by two routes: (i) perturbation theory applicable to the low force regime, and (ii) mean field theory that replaces fluctuating internal variables along the chain by their self-consistent, mean value. This latter approximation is of particular utility for the case of high chain cooperativity that suppresses strong fluctuations of the secondary structure variables. Here we provide a Ginzburg criterion[21] to discuss the limits of validity of this approximation and use Monte Carlo simulations to evaluate the response of the molecule in those regimes where the previous mean-field or perturbative approaches do not apply. We also use the Monte Carlo method to confirm our previous calculations where such analytical calculations are applicable.

This work thus explores a new range in the parameter space of the model, *i.e.* the regime of strong secondary structure fluctuations. Although estimates[19] show that at least some alpha-helical polypeptides under physiological conditions have high chain cooperativity and thus are well-approximated by the mean field description, exploring the elastic properties of a polypeptide with low chain cooperativity may well reflect the effects of poor solvent quality. In addition we will show that the model predicts that there is always a fluctuation-dominated regime near the point at which the alpha-helix denatures under tension.

To briefly review the phenomenology of the model, we find a highly nonlinear elastic response of the alpha-helix when subjected to bending torques and stretching forces as a result of the interaction between the local secondary structure and the conformational fluctuations. In particular we reported a mechanical instability of the chain under bending akin to a “buckling instability” in which the segment of alpha-helical polypeptide locally melts to form a denatured (random coil) segment beyond a critical angle. At this point the torque required to hold the chain at that particular angle drops precipitously.

Upon application of a tensile stress to an alpha-helical polymer we find three regimes of response. At the lowest stresses, the external force pulls out the small equilibrium undulations of the stiff alpha-helical polymer in a manner identical to the WLC. There are however, significant differences between the force extension behaviors of the WLC and the HCWLC. In the WLC model the extensional compliance of the chain vanishes in the limit of large forces because each segment of the chain is inextensible. The applied tensile force simply depletes the equilibrium population of transverse undulations along the chain. As these undulations vanish no additional arc

length can be recovered by additional force; the measured extension of the chain plateaus at its total contour length. This is not the case for the HCWLC. For short enough chains (to be quantified below) the standard Marko-Siggia plateau in which additional force does not produce extension is replaced by what we term a “pseudoplateau” characterized by the fluctuations of the polymer into the random coil, or denatured state. Since the random coil sections of the chain are longer than the same segments in their native, alpha-helical state, the biasing of the fluctuations into the random coil leads to additional contour length of the polymer. Finally in the third regime the chain is completely denatured by the applied force and reaches a true Marko-Siggia plateau upon further increasing the force.

The remainder of the paper is organized as follows. In section II we introduce the alpha-helix Hamiltonian based on a combination of the worm-like chain and the helix/coil model. The details of the Monte Carlo simulation is described in III. The simulation results are analyzed in the section IV. We first study the radius of gyration of the alpha helix as a function of solvent quality (to be defined therein) in section IV A. We then examine the response of the chain to bending torques in section IV B 1. In section IV B 2 we study the extensional compliance of the alpha-helix before summarizing and discussing the results in section V.

## II. THE HELIX-COIL WORM-LIKE CHAIN MODEL

The worm-like chain (WLC)[1, 2] is the simplest coarse-grained model for semiflexible polymers. This model describes the single-chain polymer statistics in terms of a Hamiltonian that associates an energy cost with chain curvature by introducing a bending modulus  $\kappa$ . In terms of a discretized chain model described by the set of monomeric tangent vectors  $\hat{t}_i$ ,  $i = 0, \dots, N-1$  with  $N$  the degree of polymerization, the WLC Hamiltonian may be written as

$$H_{\text{WLC}} = \kappa \sum_{i=0}^{N-1} [1 - (\hat{t}_i \cdot \hat{t}_{i+1})]. \quad (1)$$

The bending modulus  $\kappa$  determines the thermal persistence length of the chain, the typical distance along the chain over which the tangent vectors decorrelate.

The response of a single chain to extensional forces has been used to understand the deformational properties of biopolymers and their aggregates[12, 22, 23]. To account for the internal degrees of freedom along the chain a new set of variables is needed. Workers have previously employed the helix/coil (HC) model[24] in order to introduce such internal state variables along the arc length of the chain. This model has been used to study a class of protein conformational transitions[25, 26] in solution and under tension[27].

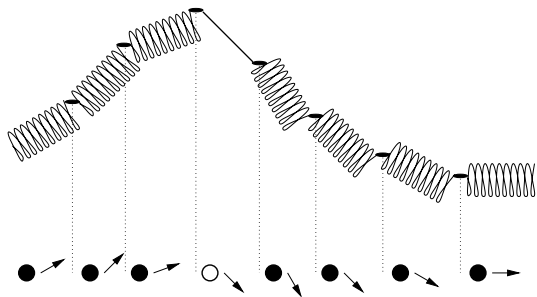


FIG. 1: Schematic figure of an alpha-helical polypeptide and its representation in terms of the Ising-like secondary structure variables (open circles for random coil segments and filled ones for alpha-helical ones) and the tangent vectors to the segments of the chain (denoted by arrows).

The HC model Hamiltonian, which is used to study these structural transitions can be reduced to its simplest form by assuming that the local structure of the chain can be described by a set of two-state variables  $s_i = \pm 1$ ,  $i = 0, \dots, N$ . For the alpha-helical chains of current interest we regard these two states as the local conformation of the segment in its native, alpha-helical state ( $s = +1$ ) and in a disordered, random coil state ( $s = -1$ ).

It is important to note that the elementary units of the chain as described by the HCWLC model are not the amino acid monomers but rather turns of the alpha helix since it is necessary to unambiguously ascribe the presence or absence of secondary structure to each elementary unit of the model. In practice we expect this level of coarse graining to mean that each segment of the chain (or elementary unit) is composed of  $\sim 3$  monomers.

The coupling of the secondary structure variables to the WLC tangent vectors is effected by introducing a bending stiffness in the WLC Hamiltonian that depends on the local degree of secondary structure. We choose

$$\kappa(s) = \begin{cases} \kappa_{>} & \text{if } s = +1 \\ \kappa_{<} & \text{if } s = -1 \end{cases} . \quad (2)$$

Due to the hydrogen bonding between turns of the alpha-helix, it is reasonable to expect that  $\kappa_{>}$  the bending modulus in the native state is significantly larger than  $\kappa_{<}$  the bending modulus of the chain in the non-native, disordered state. Simple estimates of this difference in bending moduli were computed in [19].

The Hamiltonian of the helix-coil worm-like chain may be thus written as

$$H = \epsilon_w/2 \sum_{i=0}^{N-1} (1 - s_i s_{i+1}) - h/2 \sum_{i=0}^N (s_i - 1) + \sum_{i=0}^{N-1} \kappa(s_i) [1 - (\hat{t}_i \cdot \hat{t}_{i+1})], \quad (3)$$

where  $\epsilon_w$  is the free energy cost of a domain wall in the secondary structure sequence and is the negative natural

logarithm of the chain cooperativity parameter;  $h$  represents the free energy cost per monomer to be in the non-native (*i.e.* random-coil) state, while  $\kappa_{>}$  and  $\kappa_{<}$  are the bending moduli of the chain in the helix and coil phases as mentioned above. A pictorial representation of the system is shown in figure 1.

The full Hamiltonian given by Eq. 3 has four constants with dimensions of energy:  $\kappa_{>}, \kappa_{<}, h, \epsilon_w$  that can be fit from experiment. We have disregarded the twist degree of freedom of the molecule. Such twist degrees of freedom and the coupling of twisting and stretching modes of these chiral molecules have been explored particularly with regard to the mechanical properties of DNA[28, 29]. Also in the present work we evaluate the model in two dimensions. Full three dimensional variants of the calculation that incorporate torsional modes as well as the twist-stretch coupling are currently under investigation[30].

### III. MONTE CARLO SIMULATIONS

We performed Monte Carlo simulations of the helix coil worm-like chain model using a standard Metropolis algorithm. Our system consists of a linear chain of  $N$  lattice points with two variables specified at each lattice position, a scalar variable  $s_i = \pm 1$  recording the presence or absence of secondary structure and an angular variable  $\theta_i$  specifying the angle the tangent vector joining two sites of the chain make with the mean direction. The number of tangent vectors in the simulation is one less than the total number of spins, *i.e.* it is  $N - 1$ .

The energy of the chain is specified by the Hamiltonian given by Eq. 3. We choose for our initial configuration a state having equal numbers of helix and coil segments and with randomized tangent vectors. There are two classes of Monte Carlo moves: spin flips representing attempts to change the local secondary structure and tangent vector moves allowing the chain to explore all conformations. To update the configuration of the chain, we flip a spin at random  $s_i \rightarrow -s_i$  and calculate the energy difference between the final ( $\nu$ ) and the initial configurations ( $\mu$ ). The acceptance probability of this move is given by

$$A(\mu \rightarrow \nu) = \begin{cases} \exp[-\beta(E_\nu - E_\mu)], & E_\nu - E_\mu > 0 \\ 1 & \text{otherwise} \end{cases} , \quad (4)$$

where  $\mu$  and  $\nu$  represent the initial and final state of the system respectively.

In the next sweep of the lattice we pick  $\theta_i$  at random, attempt a Monte Carlo update of an angular variable  $\theta_i \rightarrow \theta_i \pm \Delta\theta$  and accept or reject it according to the Metropolis algorithm outlined above. We find that choosing  $\Delta\theta = 0.01$  allows us to equilibrate the chain over reasonable timescales while being small enough so that the discretization of chain conformations does not significantly affect the numerical results. This latter point was checked by a comparison to runs with even smaller values of the angular variable updates. We study systems of sizes ranging from  $N = 10$  to  $N = 100$ . We see a small

but finite system-size dependence in the sharpness of the transitions of the underlying spin variables.

Finally, because of their discrete nature the spin variables equilibrate much faster than the angular variables. In all the runs we checked that we had performed a sufficient number of Monte Carlo steps in order to equilibrate the largest correlated structures in the system that have the slowest dynamics, *i.e.* the equilibration time  $\tau_{\text{eq}}$  was always taken to be greater than  $4\tau_{\text{cor}}$  – the largest correlation time in the system. Due to the wide separation of the time scales for the equilibration of the helix–coil and angular variables, a more efficient Monte Carlo scheme could be developed by updating the angular variables more often than the secondary structure variables when deep in the ordered phase of these secondary structure variables. We did not pursue such improvements of the efficiency of the code there.

We benchmarked our code by comparing our results to the known equilibrium properties of the Ising model and the Kratky-Porod model in the limit where we have artificially frozen either the tangent vectors or the spin variables respectively. In these cases the HCWLC model reduces to these well-studied cases.

As an example of these checks of the numerics we first examine the WLC limit of the model by fixing the secondary structure variables  $s_i = +1$  for all  $i$ . In this limit, the HCWLC Hamiltonian is given by Eq. 1 up to a trivial constant. The correlation function for this WLC Hamiltonian can be calculated exactly[2]. For our tangent vectors in two dimensions we find that

$$\langle \hat{t}_i \cdot \hat{t}_j \rangle \sim \exp[-|j - i|/l_p], \quad (5)$$

where  $l_p$  is the persistence length of the chain that is given in terms of the bending modulus by

$$l_p = -\log\left[\frac{1}{2\pi I_1(\kappa)}\right], \quad (6)$$

This length is the distance along the chain over which tangent vectors decorrelate. We have equilibrated the chain over  $2 \times 10^4$  time steps (corresponding to about 500 lattice sweeps) before making our measurements. We show in panel a) of the figure Fig.2 the dependence of the persistence length upon the bending modulus. The dashed line shows the agreement to the prediction of Eq. 6. In panel b) of the same figure we examine the Ising limit of the model in which we fix the tangent vectors to lie along the  $\hat{x}$ -axis. Here we plot the zero-temperature phase transition of the helix-coil (Ising) variables as a function of the solvent quality  $h$  (magnetic field in the Ising language). As predicted for the one-dimensional Ising model, the system jumps spontaneously to the helix phase upon making  $h$  an arbitrarily small positive quantity.

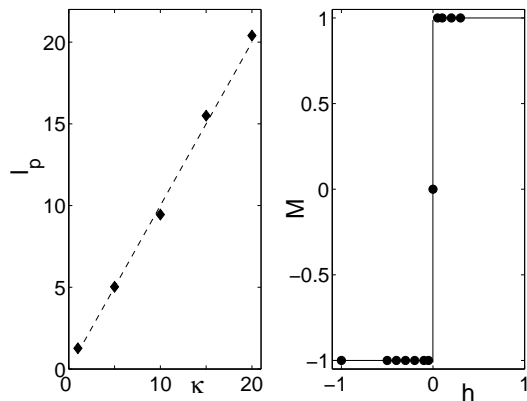


FIG. 2: a) Variation of the persistence length as a function of bending modulus of the WLC with  $\kappa$  measured in units of  $k_B T$ . b) The Ising limit of the model showing the magnetization curve:  $M$  vs  $h$  at  $k_B T = 10^{-4}$ . Both the figures are for an  $N = 20$  chain. The error bars are the size of the symbols.

## IV. RESULTS

### A. The radius of gyration

We now turn to the full HCWLC model and discuss first the radius of gyration[11]. To do so we note that the projection of the polymer arc length along the average tangent vector of a segment, *i.e.* the effective length of the segment depends on the state of secondary structure. To account for this aspect of the coarse-grained HCWLC polymer model we define a segment length that is a function of the secondary structure variable  $s_n$  via

$$\gamma(s) = \begin{cases} \gamma_< & \text{if } s = +1 \\ \gamma_> & \text{if } s = -1 \end{cases}, \quad (7)$$

where, as the notation suggests,  $\gamma_< < \gamma_>$ . The length of a segment increases when it loses its alpha-helical secondary structure. We return to a discussion of reasonable numerical estimates of these values in the conclusions.

The separation vector between the  $i^{\text{th}}$  and  $j^{\text{th}}$  segments along the chain is given by

$$\vec{R}_{ij} = \sum_{n=i}^{j-1} \gamma(s_n) \hat{t}_n, \quad (8)$$

where  $\gamma(s_n)$  is the length of the  $n^{\text{th}}$  segment measured along its mean chain tangent as defined above.

To compute the radius of gyration in our simulations we first evaluate the center of mass of the polypeptide. This is given by the expression

$$\vec{R}_{\text{cm}} = \frac{1}{N} \sum_{j=1}^N \sum_{i=1}^j \gamma(s_i) \hat{t}_i. \quad (9)$$

The radius of gyration is then evaluated by computing

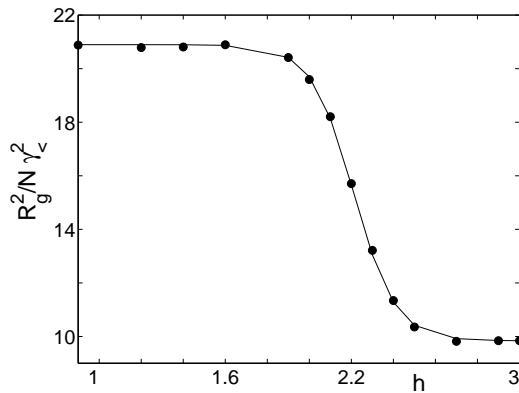


FIG. 3: Radius of gyration of the HCWLC as a function of the free energy cost per segment to transform to the random coil, nonnative state:  $h$  obtained from Monte Carlo simulations (plotted using black dots) as compared with the theory [19]. In this curve  $\kappa_{>} = 100$ ,  $\kappa_{<} = 1$ ,  $N = 10$ , and  $\epsilon_w = 10$ . All the energy scales are measured in  $k_B T$  and the error bars are smaller than the symbols in the plot.

the average

$$R_G^2 = \frac{1}{N} \left\langle \left( \sum_{j=1}^N \left( \sum_{i=1}^j \gamma(s_i) \hat{t}_i - \vec{R}_{\text{cm}} \right) \right)^2 \right\rangle. \quad (10)$$

We plot in Fig. 3 the radius of gyration as a function of  $h$  for  $\epsilon_w = 10$ , and bending moduli  $\kappa_{>} = 100$ , and  $\kappa_{<} = 1$  for an  $N = 10$  sized chain obtained using Monte Carlo simulations (black dots). These data are in excellent agreement with our analytic calculations (solid line). The energy scale  $h$  is the free energy cost of a segment being in its nonnative (*i.e.* random coil) state and so variations of  $h$  mimic changing the solvent quality as is done in the denaturation of proteins by the addition of *e.g.* Guanidinium[31]. A second effect of solvent quality is the change in the effective excluded volume interaction between segments of the polymer. This is not included here but, since the chain never approaches a random coil configuration in these simulations we expect that the absence of self-avoidance plays a minimal role in the above results.

Similar behavior is seen in the dependence of the squared averaged end-to-end vector of the chain. For high chain cooperativities and  $h$  chosen so that the chain is in either the all helix or all coil phase we find this quantity has the following expected scaling form for a worm-like chain:  $\Delta R^2 = N^2 \gamma^2 g(\frac{N\gamma}{l_p})$ , where we have introduced the function:  $g(x) = 2(\exp[-x] - 1 + x)/x^2$  and  $\gamma$  is either  $\gamma_{>}$  or  $\gamma_{<}$  for the all helix or all coil chains respectively. The behavior of the HCWLC is similar to the WLC but with a persistence length that interpolates between that of the helix and the random coil. This results also agrees with previous analytic calculations[19].

## B. Mechanical Properties

### 1. Torque response

To begin our numerical exploration of the mechanical properties of the model, we consider the response of the chain to externally applied torques in thermal equilibrium. These torques act to constrain the tangent vectors of the ends of the molecule while not applying tensile stress. Since the restricted partition function of the chain with arbitrarily fixed end tangents can be computed exactly, we expect the results of the simulations to agree with the previous work for all values of the model parameters. The response of the chain to tensile stress or to the combination of tensile stress and bending torques, however, cannot be computed analytically in closed form; it is there that the complementary utility of the Monte Carlo approach will be seen.

To study the torque response of the chain, we hold the first tangent vector fixed along the  $\hat{x}$ -axis and constrain the last chain tangent to make a fixed angle  $\psi$  with respect to the same axis. We numerically evaluate the constraining torque  $\tau(\psi)$  by computing the derivative of the free energy with respect to the angle  $\psi$ . In our simulations this is effected by directly calculating the thermal average:

$$\tau(\psi) = \langle \kappa(s_{N-1}) \sin[\psi - \theta_{N-1}] \rangle. \quad (11)$$

The results, which corroborate the analytic calculations are plotted in figure 4. At small values of the bending angle  $\psi$ , there is a linear dependence of the constraining torque on  $\psi$ . The alpha-helix bends like a flexible, elastic rod. At a certain critical angle  $\psi^*$ , however, the constraining torque reaches a maximum and then drops precipitously for angles  $\psi > \psi^*$  as shown in figure 4. This dramatic collapse of the chain's rigidity is akin to the buckling instability of a macroscopic tube such as a drinking straw. The mode of the localized failure though is quite different. In the case of current interest, the failure is caused by the localized disruption of the secondary structure. The breaking of the hydrogen bonds at this denatured site introduces a weak link allowing the molecule to bend at a lower torque. At  $\psi = \psi^*$ ,  $M$ , the fraction of the chain in the nonnative state, abruptly jumps to  $\mathcal{O}(1/N)$  demonstrating that, within the model, the buckling failure is due to the creation of a single random coil segment along the chain that provides a region of greatly reduced bending stiffness. The size of the created random-coil section will remain on the order of  $N\kappa_{<}/\kappa_{>}$  so for a large difference in bending moduli between the native and nonnative states of the chain, these "weak links" generically occupy a small fraction of the polymer. For instance, in the example shown in figure 4 there is only one weak link created.

The above behavior is seen in the parameter range ( $\epsilon_w$ ,  $h$ ) consistent with the chain being in an all helix state in thermal equilibrium in the absence of applied torque.

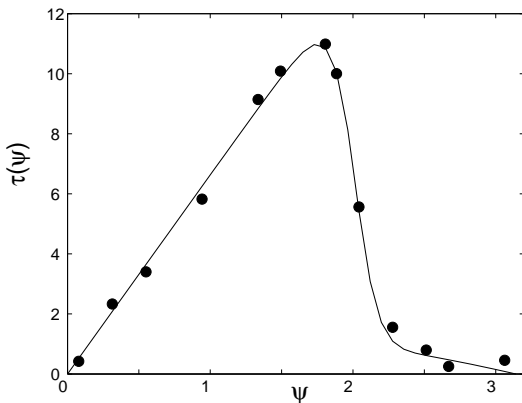


FIG. 4: Numerical torque vs. angle data (filled points) for  $\epsilon_w \approx 5.2$ ,  $h = 8$ ,  $\kappa_> = 100$ , and  $\kappa_< = 1$  compared with previous exact calculations [13,14] (solid line) for an  $N = 10$  chain. The torque is measured in units of  $k_B T$ . The error bars are of the same size as the symbols in the plot.

If the equilibrium system is in a mixed helix-coil phase such a behavior is not observed. Instead we see a monotonic increase in the bending torque for all end angles less than  $\pi$  as expected for an elastic rod. At  $\psi = \pi$  the torque measured in thermal equilibrium is identically zero since one is averaging a signed quantity and the statistical weight of positive and negative torques becomes equal. The average of the squared torque, however, vanishes only at  $\psi = 0$  modulo  $2\pi$ . Since it is reasonable to suppose that the chain bends in the plane defined by first and last constrained chain tangents, one expects that our two-dimensional results accurately captures the buckling instability of the chain. We expect that the full three dimensional calculation would generate at least qualitatively similar results.

We now turn to the numerical study of the extensional compliance of the chain. These Monte Carlo simulations complete the analysis of extensional compliance of the model by accessing parameter regimes where neither of our previous approximations are valid. In particular we look at the extensional compliance where the mean field approximation fails and we look at the modification of the extensional compliance due to applied torque. The existence of this torque/stretch coupling is due to the inherent nonlinearity of the model.

## 2. Extensional compliance

In the presence of a tensile force  $F$ , the Hamiltonian of the HCWLC may be written as

$$H = H_0 - F \sum_{i=0}^N \gamma(s_i) \cos(\theta_i), \quad (12)$$

where  $H_0$  is the HCWLC Hamiltonian in the absence of externally applied forces as shown in Eq. 3. In our Monte

Carlo simulations we apply a force of magnitude  $F$  and then equilibrate the chain as described above. We then calculate the quantity

$$L(F) = \left\langle \sum_{i=1}^N \gamma(s_i) \hat{t}_i \right\rangle. \quad (13)$$

This result gives the mean length of the chain as a function of the externally applied force. Similar measurements are made for the case where the initial and final chain tangents are constrained:  $\theta_1 = 0$  and  $\theta_N = \psi$ . These latter simulations allow us to explore the nonlinear dependence of the extensional compliance upon applied torque. In such simulations we compute

$$L(F, \psi) = \left\langle \sum_{i=1}^N \gamma(s_i) \hat{t}_i \right\rangle \Bigg|_{\theta_0=0, \theta_N=\psi}. \quad (14)$$

In all the extension measurements the force is always collinear with the initial chain tangent,  $\hat{t}_1 = \hat{x}$ .

We plot in figure 5 the force-extension curve of the HCWLC model with two sets of parameter values. In both force extension measurements we do not constrain the final chain tangents and numerically determine the function defined in Eq. 13. In the first case (upper panel of the figure) we have selected the HCWLC model parameters such that the polymer is in a fluctuation-dominated regime where the mean-field approximation is not valid. In the lower panel we have tuned those parameters to suppress secondary structure fluctuations.

In upper panel we take  $\epsilon_w = 0.5$  and  $h = 1.0$  to enhance the secondary structure fluctuations. The bending moduli are chosen to be  $\kappa_> = 4$  and  $\kappa_< = 2$  respectively. Here we do not expect the mean field theory (shown as a solid line in figure 5) to fit the simulation data. The mean field theory indeed fails to describe the force extension curve adequately. In particular we note that the most significant discrepancy between the mean-field theory and the data occurs at low forces. In the limit of high forces, the tension in the polymer acts as an ordering field suppressing the fluctuations that the mean-field theory ignores. Moreover, we note that the intermediate plateau (“pseudoplateau”) in the graph of extension vs. applied force vanishes for this parameter regime. We return to the vanishing of the pseudoplateau below. In fact in the limit of low chain cooperativity, the polymer is typically found in a mixed helix/coil phase and we obtain force extension curves similar to those the WLC results of Marko and Siggia[12].

In the limit of high chain cooperativity (simulation data and mean field prediction shown in the lower panel of figure 5), the data agree well with our previous mean-field calculations using the HCWLC model as expected. In this case we have taken  $\epsilon_w = 8$  to enforce high chain cooperativity and suppress secondary structure fluctuations. We have taken the remaining parameters to be  $h = 1.5$ ,  $\kappa_> = 100$  and  $\kappa_< = 1$ .

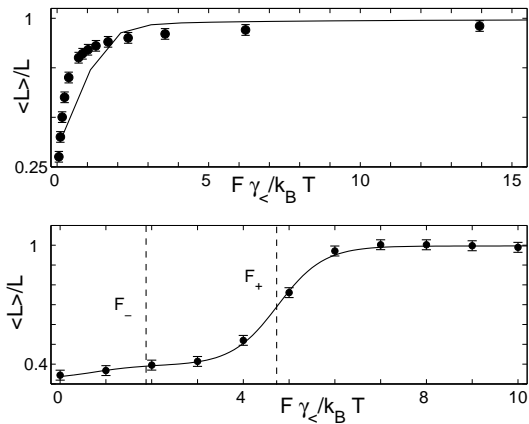


FIG. 5: Force vs. extension Monte Carlo data (points) shown in the low (upper panel) and high (lower panel) cooperativity limit. In each the mean length of the chain normalized by the maximum chain length  $N\gamma_>$  is plotted as a function of the applied force normalized by the length of a helix segment  $\gamma_>$ . For the upper panel the parameters are  $\epsilon_w = 0.5$ ,  $h = 1.0$ ,  $\kappa_> = 4.0$ ,  $\kappa_< = 2.0$ , and  $N = 20$ . The lower panel the parameters are  $\epsilon_w = 8$ , and  $h = 1.5$ , and  $\kappa_> = 100$ ,  $\kappa_< = 1$ , and  $N = 10$ . In both graphs the mean field calculation [19] is shown as a solid line.

Returning to the appearance of the pseudoplateau in the upper panel of figure 5 we recount the explanation of its existence. For small applied forces, a molecule in the all-helical phase having large stiffness approaches its maximum length  $N\gamma_<$  as  $1/\sqrt{\frac{F\kappa_>\gamma_<}{k_B T}}$ . The WLC predicts the vanishing of the extensional compliance as the chain reaches its maximal length; this would produce a plateau at these intermediate forces. This plateau, however, is not flat in the HCWLC due to the fact that an increase in the applied force enhances the fluctuations into the longer, random coil phase of the segments, which we refer to as the pseudoplateau. The end of this plateau is marked by a sharp lengthening transition at a value of force  $F_+ \approx \frac{\epsilon_w + h}{\Delta\gamma}$  where  $\Delta\gamma = \gamma_> - \gamma_<$ . Here we observe the force-induced denaturation of helical domains.

Upon closer examination one notes that the appearance of this intermediate-force pseudoplateau is actually a finite-size effect in the model. The width of this pseudoplateau is controlled by two forces, a force at onset  $F_-$  and a maximum force  $F_+$  at which point the abrupt denaturation transition occurs. These forces are marked on figure 5. The lower force  $F_-$  is determined by the beginning of the first Marko-Siggia plateau where the amplitude of transverse thermal undulations of the all-alpha-helical polymer have been significantly reduced. Because that reduction has an algebraic dependence on applied force, it is not possible to unambiguously select a critical force marking the onset of the plateau. It appears reasonable, however, to insist that plateau has been reached when  $dL/dF (1/\gamma_<^2) \ll 1$ , *i.e.* the when the incremental extension of the chain measured in monomer lengths  $\delta L/\gamma_<$  is small for a change in force  $\delta F \sim 1/\gamma_<$  set by the

thermal energy ( $k_B T = 1$ ) divided by the same monomer size. In this case we find the force associated with the plateau onset  $F_- \sim N^{2/3} \kappa_>^{-1/3} \gamma_<^{-1}$  grows with the length of the chain. Longer chains require larger forces to sufficiently pull out the equilibrium population of transverse undulations and thereby reach the plateau regime.

The high force end of the plateau is determined by balancing the free energy cost associated with transforming a segment from alpha helix to random coil with the work done by the external force during that transformation:  $h + \epsilon_w \sim \Delta\gamma F_+$ . On the left hand side is the free energy cost of making one domain wall and converting one segment to the thermodynamically unfavored random coil state. The right hand side of the same relation gives the work done by the external force as one segment lengthens by  $\Delta\gamma$ . The existence of the pseudoplateau requires that  $F_- < F_+$ ; the applied force must straighten out the alpha helix at tensions small enough such that the force-induced helix-to-coil transition does not occur. This final inequality demands that

$$N \leq \left( \frac{h + \epsilon_w}{\gamma_< \Delta\gamma} \right)^{3/2} \kappa_>^2. \quad (15)$$

Typical alpha helical polypeptides are quite short  $N \sim \mathcal{O}(10)$  and stiff  $\kappa_> \sim \mathcal{O}(10^2)$  so that one expects to observe this pseudoplateau behavior quite generally. We see that for the parameters used to create the upper panel of figure 5 the criterion for the presence of the pseudoplateau is not met and in our Monte Carlo simulations we indeed observe no pseudoplateau for these values. When the criterion is met as in the case shown in the lower panel of figure 5, the mean field example, the pseudoplateau is evident.

We now consider the force extension measurements made while constraining the initial and final chain tangents. In this manner we compute the mean extension as a function of applied force as well as the imposed total angular bend on the polymer. This quantity is defined by Eq. 14. In the regime where the persistence length of the chain in both the helix and the coil states is smaller than the chain itself, these constraining torques have essentially no impact on the extensional compliance of the chain. The effect of the angular constraints is limited to boundary regions within a persistence length of the constrained ends. For stiffer chains having a persistence length longer than the chain itself, there is a significant nonlinear coupling between these constraining torques and the extensional compliance of the polymer at low to moderate forces.

Such effects are shown in figure 6 where we plot two force extension curves for a HCWLC having parameters  $\kappa_> = 40$ ,  $\kappa_< = 2$ ,  $\epsilon_w = 8$  and  $h = 1.5$ . In both cases the initial chain tangent is constrained to lie along the  $\hat{x}$ -axis, the direction of the tensile force. In one case (triangles) the final chain tangent is collinear with the initial chain tangent, while in the second case (circles) the final chain tangent makes an angle  $\psi = \pi/2$  with the initial one. These simulations numerically evaluate

the thermal average of the chain's extension as defined in Eq. 14 with  $\psi = 0, \pi/2$ .

At low applied force we see that, due to the nonlinear coupling of applied torque and force, the chain has a greater extensional compliance in the bent state. The  $\psi = \pi/2$  chain reaches its pseudoplateau more rapidly with increasing force. Once the chain denatures under the tensile stress causing the persistence length to become shorter than the chain itself, the coupling between the extensional compliance and end tangent constraint disappears. As one approaches arbitrarily high forces the effect of the constrained end tangent itself becomes localized at the last segment of chain regardless of the bending moduli of the polymer so that its effect becomes negligible. In the limiting case of infinite force there remains only the effect of the constrained end itself, which decreases the length of the chain by  $\gamma > (1 - \cos \psi)$ . In the strongly fluctuating secondary structure regime, we have not been able to extract any systematic information about the nonlinear coupling of force and torque for low forces.

The numerical calculation presented here does not directly probe the force/torque coupling since we have measured the extensional compliance in an ensemble of chains with fixed end tangents. We have directly measured the function defined by Eq. 14. Clearly, the constraint torques applied to the end have a complicated dependence on the extensional stress. In order to quantitatively probe the force-torque coupling it is necessary to work in a fixed torque ensemble rather than a fixed angle one. The results presented here may, however, directly apply to protein mechanics where allosteric rotations of the final tangents of an alpha helical domain can directly modify the extensional elasticity of the helix thus affecting both its mean length and fluctuation spectrum.

Returning to the observed breakdown of the mean field theory for the force extension curves, we ask can one develop a simple criterion to predict the region of HCWLC parameter space where our analytic mean field analysis will hold? Indeed from the energy fluctuations observed in the Monte Carlo simulation one can directly map the boundaries of the fluctuation-dominated regime. It is clearly desirable to develop a criterion that can be written directly in terms of the model parameters so that one may know immediately where the simpler analytic theory applies.

We observe that if the polymer were straight the effect of the force on the remaining secondary structure variables would be to simply shift the effective free energy cost per segment to destroy the secondary structure from  $h$  to  $h_{\text{eff}} = h - F\Delta\gamma$ ; the cost of denaturing the segment is  $h$  but the net work done by the chain upon extension under the external force  $F$  is  $-F\Delta\gamma$ . We recall that the validity of the mean field theory requires only the suppression of secondary structure fluctuations. We then expect that mean field theory to fail where  $h_{\text{eff}} = h - F\Delta\gamma$  is small, which for reasonable values of  $h$  requires significant forces. Assuming that these forces have quenched

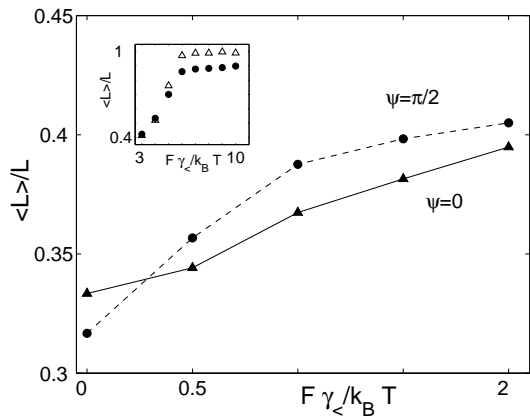


FIG. 6: Force vs. extension curves for HCWLC chain with constrained end tangents. The force vs. extension is shown for chains where the first tangent lies along the direction of the pulling force while the second tangent makes an angle of  $\psi = 0$  (triangles) or  $\psi = \pi/2$  (circles) with respect to the initial chain tangent. The parameters of the chain are:  $\kappa_{>} = 40$   $\kappa_{<} = 2$ ,  $\epsilon_w = 10$ ,  $h = 1$ , and  $N = 20$ . Note the extensional compliance depends on the state of the final chain tangent. The inset shows that the chain extension in the direction of applied force saturates at high forces to different values as a result of the constrained end tangent.

most of the contour fluctuations of the chain, we take as an approximate criterion for the breakdown of mean field theory the Ginzburg criterion for the one-dimension helix-coil model with an effective field  $h_{\text{eff}}$ . Thus mean field theory is expected to hold when

$$\frac{\langle s_i^2 \rangle - \langle s_i \rangle^2}{\langle s_i \rangle^2} \ll 1. \quad (16)$$

Neglecting boundary effects to restore the translational invariance along the chain and taking  $N$  large enough so that we may consider only the  $\lambda_1$ , larger of the two eigenvalues of the transfer matrix, this condition can be written as

$$\frac{\lambda_1(\partial^2 \lambda_1 / \partial h^2)}{(\partial \lambda_1 / \partial h)^2} \ll 1 \quad (17)$$

where the larger eigenvalue, computed in [19] is given by

$$\lambda_1 = (1 + e^{-h_{\text{eff}}}) + \frac{1}{2} \sqrt{(1 - e^{-h_{\text{eff}}})^2 + 4 \exp[-2\epsilon_w - h_{\text{eff}}]}, \quad (18)$$

where  $h_{\text{eff}}$  is defined above.

We determined the boundary marking the limits of validity of the mean field theory in the parameter space spanned by  $\epsilon_w$  and  $h_{\text{eff}}$  is shown in Fig.7. To the right of the dots mean field theory holds while in the region to the left of this division the system is dominated by large secondary structure fluctuations. Two traces of total energy as a function of Monte Carlo time representative of each region are shown as insets. In figure 7



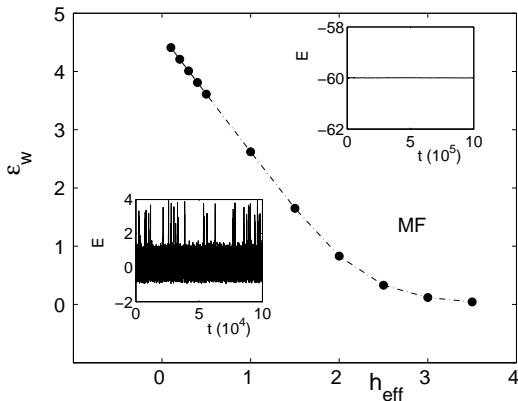


FIG. 7: A map of the  $\epsilon_w - h_{\text{eff}}$  parameter space of the helix coil degrees of freedom showing the region of validity of the mean field approximation (MF) as determined by the Ginzburg criterion. The insets show the energy fluctuations over Monte Carlo steps in numerical simulations of the two regimes.

the filled points represent the boundary at which the energy fluctuations reach one part in  $10^3$  of the mean. The Ginzburg criterion defined by Eq. 17 give the dashed line when the left hand side of Eq. 17 is also taken to be  $10^{-3}$ . The correspondence of the Ginzburg criterion and the Monte Carlo fluctuation data demonstrates the utility of this measure of the validity of the mean field approximation. The Ginzburg criterion as described above correctly distinguishes these two regimes. From that figure it is clear that mean field theory holds in the limit of high chain cooperativity as expected. We note, however, that since the force-induced denaturation of the chain requires  $h_{\text{eff}} \rightarrow 0$  we expect that at this transition there will be significant fluctuation effects. Such effects have not been fully explored.

## V. CONCLUSIONS

We have numerically explored the nonlinear elastic response of the helix/coil worm-like chain under applied forces and torques. Our Monte Carlo simulations of the extensional compliance of the polymer agree satisfactorily with previous analytic calculations in two limits: (i) for small forces our results are consistent with perturbative calculations, and (ii) where mean field theory is expected to hold as determined by a Ginzburg criterion, we find that our mean field analysis is consistent with the Monte Carlo data. It should also be noted that the response of the polymer to applied torque agrees with the analytic calculations; this is to be expected as the force-free partition function of the system can be computed exactly in closed form.

The appropriate energy scales  $h$  and  $\epsilon_w$  to describe typical alpha-helical polypeptides under physiological conditions can be estimated to be  $h \approx 1.5$  and  $\epsilon_w \approx 7$  [32, 33].

For such parameters and polypeptides of no more than  $N \sim \mathcal{O}(10)$  turns it appears from our Ginzburg criterion that the chain is typically well-described by the previous mean field approximation. Nevertheless in order to understand the statistical mechanics of force-induced denaturation of long polypeptides where  $\Delta\gamma F \sim h$  or the denaturation via changes in solvent quality so that  $F = 0$  and  $h, \epsilon_w \rightarrow 0^+$  one must study the fluctuation dominated regime that is accessible via Monte Carlo. In this fluctuation-dominated regime we find that the extensional behavior is well described by the Marko Siggia description of the WLC with a persistence length that interpolates between its value in the helix and coil states. In that regime the pseudo-plateau is absent. Such Monte Carlo calculations can, in effect, probe the unfolding transition state for such force-induced unfolding within the current model. By further developing the model and studying these transition states one may be able to assess the role of chain cooperativity in the unfolding process. A better understanding of this point should help to elucidate constant velocity, single-protein unfolding experiments.[34, 35].

Moreover the Monte Carlo calculations provide a non-perturbative approach to investigating the nonlinear coupling between response of the chain to combinations of applied tensile forces and bending torques. Previously we had studied such nonlinear couplings only in the limit of small forces. Our new results discussed above allow us to explore the high force regime and reveal that at high forces torque plays little role in determining the extensional compliance of the molecule. However at low forces and for stiff chains such that the persistence length of the helical segments is comparable to, or larger than the length of the chain, the torque plays an important role. Such high force couplings may play a role in understanding protein conformational change.

Taken in combination with the previous analytical treatments, these Monte Carlo calculations provide a nearly complete description of the mechanical properties of the HCWLC model for alpha-helical polypeptides. It remains only to develop a full, three-dimensional description of the polymer that incorporates the torsional degrees of freedom to the problem as well as to address the role of chemical heterogeneity in order to develop a complete and rather general equilibrium description of these biopolymers.

## Acknowledgements

BC and AJL thank Prof. J. Machta for stimulating conversations regarding this work. BC also thanks Prof. N. Prokofev and B. Svitsunov for helpful discussions and for the use of computational resources. BC acknowledges the hospitality of Indian Institute of Science, Bangalore and AJL acknowledges the National Central University, Taiwan where parts of this work were done.

- 
- [1] O. Kratky and G. Porod, *Rev. Trav. Chim.* **68**, 1106 (1949).
- [2] M. E. Fisher, *Am. J. Phys.* **32**, 343 (1963).
- [3] S. Smith, L. Finzi, and C. Bustamante, *Science* **258**, 1122 (1992).
- [4] T. T. Perkins, S. R. Quake, D. E. Smith, and S. Chu, *Science* **264**, 822 (1994).
- [5] T. T. Perkins, D. E. Smith, R. G. Larson, and S. Chu, *Science* **268**, 83 (1995).
- [6] P. Cluzel, A. Lebrun, C. Heller, R. Lavery, J.-L. Viovy, D. Chatenay, F. Caron, *Science* **271**, 792 (1996).
- [7] T. Strick, J. Allemand, D. Bensimon, A. Bensimon, and V. Croquette, *Science* **271**, 1835 (1996).
- [8] T. T. Perkins, D. E. Smith, and S. Chu, *Science* **276**, 2016 (1997).
- [9] C. Bustamante, Z. Bryant, and S. B. Smith, *Nature* **421**, 423 (2003).
- [10] T. R. Strick, M.-N. Dessinges, G. Charvin, N. H. Dekker, J.-F. Allemand, D. Bensimon and V. Croquette, *Rep. Prog. Phys.* **66**, 1 (2003).
- [11] H. Benoit, and P. M. Doty, *J. Chem. Phys.* **57**, 958 (1953).
- [12] J. F. Marko and E. Siggia, *Macromol.* **28**, 8759 (1995).
- [13] M. Rief, H. Clausen-Schaumman, and H. E. Gaub, *Nat. Struct. Biol.* **6**, 346 (1990).
- [14] T. Cloutier and J. Widom, *Mol. Cell.* **14**, 355 (2004).
- [15] P. Wiggins, R. C. Phillips, and P. Nelson, *cond-mat/0409003*.
- [16] M. Zhang and T. Yuan *Biochim. Biol. Cell.* **76**, 313 (1998); J. S. Mills, and J. D. Johnson, *J. Biol. Chem.* **260**, 15100 (1985); B. F. Volkman, D. Lipson, D. E. Wemmer, and D. Kern, *Science* **291**, 2429 (2001).
- [17] W. Wriggers, E. Mehler, F. Pitici, H. Weinstein, and K. Schulten *Biol. J.* **74**, 1622 (1998).
- [18] A. J. Levine, *cond-mat/0401624* (submitted to *Phys. Rev. Lett.*).
- [19] B. Chakrabarti, and A. J. Levine, *cond-mat/0405382* (submitted to *Phys. Rev. E*).
- [20] C. Storm and P. C. Nelson, *Phys. Rev. E.* **67**, 051906 (2003).
- [21] P. M. Chaikin, and T. C. Lubensky *Principles of condensed matter physics*, (Cambridge University Press, 1998).
- [22] F. C. MacKintosh, J. Käs, and P. A. Janmey *Phys. Rev. Lett.* **75**, 4425 (1995).
- [23] A. Lamura, T. W. Burkhardt, and G. Gompper, *Phys. Rev. E.* **64**, 061801 (2001).
- [24] D. Poland, and H. A. Scheraga *Theory of helix-coil transitions in biopolymers; statistical mechanical theory of order-disorder transitions in biological molecules* (Academic Press, New York, 1970).
- [25] T. M. Birshtein and O. Ptitsyn, *Conformations of Macromolecules*, (Wiley, New York, 1966).
- [26] V. A. Bloomfield, *Am. J. Phys.* **67**, 1212 (1999).
- [27] M. Tamashiro, and P. Pincus, *Phys. Rev. E.* **63**, 021909 (2001).
- [28] R. D. Kamien, T. C. Lubensky, P. Nelson, and C. S. O'Hern *Europhys. Lett.* **38** 237 (1997).
- [29] C. S. O'Hern, R. D. Kamien, T. C. Lubensky, and P. Nelson *Europhys. B* **1**, 95 (1998).
- [30] B. Chakrabarti, and A. J. Levine (work in progress).
- [31] T. Arakawa, S. N. Timasheff, *Biochemistry* **23**, 5924 (1984).
- [32] A.-S. Yang and B. Honig, *J. Mol. Biol.*, **252**, 351 (1995).
- [33] A. Chakrabartty, T. Kortemme, and R. L. Baldwin *Protein Sci.* **3**, 843 (1994).
- [34] D. A. Smith, D. J. Brockwell, R. C. Zinober, A. W. Blake, G. S. Beddard, P. D. Olmsted, S. E. Radford, *Philosophical Transactions of the Royal Society of London, Series A: Mathematical, Physical and Engineering Sciences*, **361**, 713, (2003).
- [35] E. Evans, and K. Ritchie, *Biophys. J.* **72**, 1541 (1999).